



ELSEVIER

Contents lists available at ScienceDirect

Computer Networks

journal homepage: www.elsevier.com/locate/comnet

Bounds estimation and practical stability of AIMD/RED systems with time delays

Lijun Wang^a, Lin Cai^b, Xinzhi Liu^a, Xuemin (Sherman) Shen^{c,*}^a Dept. of Applied Mathematics, University of Waterloo, Waterloo, ON, Canada N2L 3G1^b Dept. of E&CE, University of Victoria, Victoria, BC, Canada V8W 3P6^c Dept. of E&CE, University of Waterloo, Waterloo, ON, Canada N2L 3G1

ARTICLE INFO

Article history:

Received 16 June 2009

Received in revised form 10 October 2009

Accepted 15 October 2009

Available online xxxxx

Responsible Editor: L. Jiang Xie

Keywords:

Bounds estimate

Practical stability

AIMD/RED system

Time delays

ABSTRACT

The Additive Increase and Multiplicative Decrease (AIMD) congestion control algorithm of TCP deployed in the end systems and the Random Early Detection (RED) queue management scheme deployed in the intermediate systems contribute to Internet stability and integrity. Previous research based on the fluid-flow model analysis indicated that, with feedback delays, the TCP/RED system may not be asymptotically stable when the time delays or the bottleneck link capacity becomes large [3]. However, as long as the system operates near its desired equilibrium, small oscillations around the equilibrium are acceptable, and the network performance (in terms of efficiency, loss rate, and delay) is still satisfactory. In this paper, we study the practical stability of AIMD/RED system with feedback delays and with both homogeneous and heterogeneous flows. We obtain theoretical bounds of the flow window size and the RED queue length, as functions of the number of flows, link capacity, RED queue parameters, and AIMD parameters. Numerical results with Matlab and simulation results with NS-2 are given to validate the correctness and demonstrate the tightness of the derived bounds. The analytical and simulation results provide important insights on which system parameters contribute to higher system oscillations and how to set parameters (such as buffer size and queue management parameters) to ensure system efficiency with bounded delay and loss. Our results can also help to predict and control the system performance for Internet with higher data rate links multiplexed with heterogeneous flows with different parameters.

© 2009 Elsevier B.V. All rights reserved.

1. Introduction

The first congestion collapse in the Internet was observed in 1980s, although the Internet was still in its infant stage. To solve the problem, Van Jacobson proposed the Transmission Control Protocol (TCP) congestion control algorithm based on the Additive Increase and Multiplicative Decrease (AIMD) mechanism in 1988: when there is no network congestion indication (no packet loss), the TCP congestion window size is increased linearly by-one

packet per round-trip time; otherwise, it is reduced by-half. Since then, the TCP congestion control algorithm has been widely deployed in the end systems to respond to network congestion indicators and avoid congestion collapses. To support heterogeneous traffic and multimedia applications, instead of the increase-by-one and decrease-by-half strategy, a generalized AIMD controller can use a pair of parameters (α, β) to set the increase rate and the decrease ratio [17–19], and the parameter pair can be flexibly chosen according to the TCP-friendly condition [19] and the quality of service (QoS) requirements of different applications. On the other hand, to distribute the network congestion indicators fairly to all on-going flows, active queue management (AQM) [2,5], e.g., the

* Corresponding author. Tel.: +1 519 888 4567x32691; fax: +1 519 746 3077.

E-mail address: xshen@bcr.uwaterloo.ca (X. Shen).

Random early detection (RED) scheme [6,7], has been developed and deployed in the intermediate nodes. A RED-enabled router discards the incoming packets randomly when the average queue length exceeds a certain threshold (\min_{th}) and all incoming packets are discarded when it exceeds another higher threshold (\max_{th}). With the RED schemes (which has been widely deployed in the Internet core routers [8,9]), the packet loss rate of each flow is roughly proportional to its sending rate, so network transient congestion conditions can be fairly delivered to the end systems. The AIMD congestion control mechanism and the RED queue management scheme both contribute to the overwhelming success of the Internet [16].

With the rapid advances in optical and wireless communications, the Internet is becoming a more diverse system. It contains heterogeneous links with speeds varying from tens of Kbps to hundreds of Gbps, with flow round-trip delays varying from ms to seconds. It also supports various multimedia applications with different throughput, delay, and jitter requirements. It is important to understand whether the AIMD/RED system can be stable, scalable, and efficient for the more diversified Internet.

Internet stability has been an active research topic since its first congestion collapse was observed. With a fluid-flow model of the system, it has been proved that, without feedback delay, the AIMD congestion control mechanism, coupled with the RED queue management, can ensure the asymptotic stability of the system [20]. However, with a non-negligible feedback delay, the AIMD/RED system may not be asymptotically stable when the delay and/or the link capacity becomes large [3]. On the other hand, the Internet is a very dynamic system, and it can tolerate transient congestion events. In fact, TCP controlled flows aggressively probe for available bandwidth, and create transient network congestions. Practically, a concrete system is considered stable if the deviation of the motion from the equilibrium remains within certain bounds determined by the physical situation. The desired state of a system may be mathematically unstable and yet the system oscillates close enough to this state for its performance to be acceptable. To deal with such situations, the notion of *practical stability* is more meaningful. The corresponding mathematical definition below follows that of [24,25].

Definition 1. Consider the dynamic system with time delays

$$\frac{dx}{dt} = f(t, x(t), x(t - \tau_1(t)), \dots, x(t - \tau_m(t))),$$

where $x \in E^n$, $f: I \times E^n \times E^n \times \dots \times E^n \rightarrow E^n$ is continuous. Let $\tau = \sup_{i=1, \dots, m} \tau_i(t)$.

The trivial solution of the above system is said to be practically stable if given (λ, A) with $0 < \lambda < A$, we have, for any $\xi(t) \in C[[t_0 - \tau, t_0], \mathbb{R}^n]$, $\|\xi\| < \lambda$ implies $\|x(t, t_0, \xi)\| < A$, $t \geq t_0$ for some $t_0 \in \mathbb{R}_+$.

With large time delays or link capacities, the AIMD/RED system as a whole may not be asymptotically stable [3]. However, it can be practically stable. If the deviation from the equilibrium is small, the overall system efficiency can

still be high, and the packet loss rate and queuing delay can still be well bounded, i.e., the system performance is still acceptable. Therefore, the critical issue to investigate is: does the AIMD/RED system always operate in the area close to the desired equilibrium state, and what are the theoretical bounds? To answer these questions, studying system practical stability and bounds is the key, which is also the focus of this paper.

With clearly defined bounds, a system is considered practically stable. Using the fluid-flow model of the AIMD/RED system, instead of applying the Lyapunov-like method, we derive upper and lower bounds of congestion window size and queue length by directly studying the inherent properties of the AIMD/RED system. The derived bounds provide important insights on which system parameters contribute to high oscillations of the system and how to choose system parameters (such as buffer size and queue management parameters) to ensure system efficiency with bounded delay and loss. Our main findings are: (1) surprisingly, larger values of delay and link capacity will actually reduce the oscillation amplitude of window size and queue length from their equilibrium in steady state; (2) although TCP and AIMD flows can adapt their sending rates according to available bandwidth, larger number of flows leads to longer queueing delay. Thus, it is desirable to limit the number of flows in a link or promote to use more conservative AIMD parameters to bound the queueing delay and loss; and (3) if we proportionally increase the link capacity and the number of TCP or AIMD flows, the queueing delay will be slightly reduced, thanks to the multiplexing gain. Thus, AIMD/RED should be suitable in the Internet with higher bandwidth and more flows.

The remainder of the paper is organized as follows. Section 2 briefly discusses the related work. The fluid-flow models of homogeneous and heterogeneous AIMD/RED systems are introduced in Sections 3 and 4, respectively; upper and lower bounds of the systems with feedback delays are also obtained. In Section 5, numerical results with Matlab and simulation results using NS-2 are presented to validate the derived bounds, and the impacts of different system parameters on the system performance are also discussed, followed by concluding remarks in Section 6.

2. Related work

Internet stability analysis has received wide attention [1–4]. For delay-free marking scheme, the fluid-model of the AIMD/RED system has been proved to be asymptotically stable [20]. However, as pointed out in [3], the system may become asymptotically unstable in the presence of time delays. In [21,22], sufficient conditions for the asymptotic stability of AIMD/RED system with feedback delays over single and multiple bottlenecks are given. On the other hand, simulation results show that even though the system is not asymptotically stable, it oscillates around the steady state periodically. Motivated by this phenomenon, different from many previous work on the sufficient conditions for the asymptotic stability of AIMD/RED or other network control systems, in this paper, we study the practical stability of the AIMD/RED systems with both

homogeneous flows and heterogeneous flows, and derive their theoretical bounds, i.e., bounds of flows' congestion window size and intermediate systems' queue length, given the number of flows sharing the link, their AIMD parameter pairs and round-trip times (RTTs), link capacity, and RED queue parameters.

The boundedness issue has been studied in [11–13] without giving the bounds estimate, by applying Lyapunov-like method for some TCP-like congestion control algorithms. Using deterministic fluid model for studying Internet congestion control was justified in [14], and the upper bounds on the transmission rate for two kinds of TCP-like traffic was given in [10]. However, to the best of our knowledge, the theoretical bounds of window size and queue length of AIMD/RED system with homogeneous and heterogeneous flows considering feedback delays have not been reported in the literature.¹

3. Bounds and practical stability of homogeneous-flow AIMD/RED system with time delay

3.1. A fluid-flow model of Homogeneous AIMD/RED system

A stochastic model of TCP behaviors is developed using fluid-flow and stochastic differential equation analysis in [15]. Simulation results have demonstrated that this model accurately captures the dynamics of TCP. We extend the fluid-flow model for general AIMD (α, β) congestion control: the window size is increased by α packets per RTT if no packet loss occurs; otherwise, it is reduced to β times its current value. TCP is a special case of AIMD with $\alpha = 1$ and $\beta = 0.5$.

For all AIMD-controlled flows with the same (α, β) parameter pair and round-trip delay, the AIMD fluid-model relates to the *ensemble averages* of key network variables [4,15], and is described by the following coupled, nonlinear differential equations:

$$\begin{aligned} \frac{dW(t)}{dt} &= \frac{\alpha}{R(t)} - \frac{2(1-\beta)}{1+\beta} W(t) \frac{W(t-R(t))}{R(t-R(t))} p(t-R(t)), \\ \frac{dq(t)}{dt} &= \begin{cases} \frac{N(t)-W(t)}{R(t)} - C, & q > 0, \\ \left\{ \frac{N(t)-W(t)}{R(t)} - C \right\}^+, & q = 0. \end{cases} \end{aligned} \quad (1)$$

where $\{a\}^+ = \max\{a, 0\}$, $\alpha > 0$, $\beta \in (0, 1)$; $W \in [1, W_{\max}]$ is the AIMD window size (packets), and $q \in [0, q_{\max}]$ is the queue length (packets), where q_{\max} and W_{\max} denote buffer size and maximum window size, respectively. W and q in the fluid-flow model can approximate the ensemble averages of flow's congestion window size and queue length respectively in the real system. $R(t)$ is the round-trip time, C is the link capacity (packets/s), $N(t)$ is the number of AIMD flows, and $p(t)$ is the probability of a packet being dropped or marked by an intermediate system. With ever-increasing link capacity and appropriate congestion control mechanism, variation of queuing delays becomes relatively small to propagation delays. In fact, recent work [23] reveals that the variable nature of round-trip time due to queuing delay variation helps to stabilize the TCP/RED

system. Therefore, we ignore the effect of the delay jitter on the round-trip time and assume $R(t) = R$ for simplicity.

The first differential equation of system (1) describes the AIMD (α, β) window control dynamic. α/R represents the window's additive increase, whereas $2(1-\beta)W/(1+\beta)$ represents the window's multiplicative decrease in response to packet dropping or marking probability p . Since, in steady state, the AIMD flow's window size in a practical system oscillates between βW_{\max} and W_{\max} , its average window size W over a round² is $(1+\beta)W_{\max}/2$. Each time, the window size is decreased by $(1-\beta)W_{\max} = 2(1-\beta)W/(1+\beta)$. The second equation models the bottleneck queue length as simply an accumulated difference between packet arrival rate NW/R and link capacity C . $\{\cdot\}^+$ in the model guarantees that the queue length is non-negative.

Note that, in the fluid-flow model, q and W are positive and finite quantities which approximate the ensemble averages of queue length and window size in practical systems. In ergodic systems, ensemble average equals time average. The values of q and W in the fluid-flow model can be used to predict its time average over a round in a practical system. Given the AIMD window size oscillating between βW_{\max} and W_{\max} in a round, the average duration of a round equals $2(1-\beta)WR/[(1+\beta)\alpha]$.

We consider the popular Active Queue Management (AQM) scheme, RED, in system (1). With RED, the packet dropping or marking probability, p , is determined by the average queue length q_{act} :

$$p = \begin{cases} 0, & 0 \leq q_{act} \leq \min_{th}, \\ K_p(q_{act} - \min_{th}), & \min_{th} < q_{act} \leq \max_{th}, \\ 1, & q_{act} > \max_{th}, \end{cases} \quad (2)$$

where $K_p > 0$. When $q_{act} \leq \min_{th}$, $\frac{dW(t)}{dt} = \frac{\alpha}{R}$, the window size of AIMD flows will keep increasing and will not converge to any value. Thus, in the following, we will discuss the stability of this model when $q_{act} > \min_{th}$. Without loss of generality, let $q(t) = q_{act}(t) - \min_{th}$. In addition, since the queue behaves in the same way as a Drop-Tail queue once q_{act} exceeds \max_{th} , we choose \max_{th} to be sufficiently large such that $K_p(\max_{th} - \min_{th}) = 1$.

Eq. (1) is a generalized AIMD/RED congestion control model, which includes the models studied in [2,4,15]. If we choose $\alpha = 1$, $\beta = 0.5$, (1) is equivalent to the traditional TCP/RED model in [15].

The equilibrium point (W^*, q^*) for (1) and (2) is given by

$$W^* = \frac{R \cdot C}{N}; \quad q^* = \frac{\alpha(1+\beta)N^2}{2(1-\beta)R^2 C^2 K_p}.$$

Remark 1. At the equilibrium, the total arrival rate equals the total link capacity, so the link bandwidth can be fully utilized. In other words, the equilibrium point is also the most desired operating point of the system. If the window size is larger than W^* , the queue will build up which results in a longer queuing delay; if the window size is

¹ Part of this paper was presented in IEEE ICC'08.

² A round is defined as the interval between two time instants that the flow reduces its congestion window size consecutively.

less than W^* , the network load is smaller than its capacity, so the network resources are not fully utilized.

3.2. Upper bound on window size

In this section, we show that even though the system may become asymptotically unstable because of the effects of time delay, its window size and queue length are still bounded, and the upper bound of window size is close to the equilibrium.

We study the delayed homogeneous AIMD system defined by (1) with RED defined by (2) and derive the upper and lower bounds of the system. We set $\min_{th} = 0$ in RED and assume that the traffic load (i.e., the number of AIMD flows) is time-invariant, i.e., $N(t) = N$. As mentioned earlier, we ignore the effect of the delay jitter on the round-trip time and derive the bounds of AIMD/RED system assuming RTT to be constant. Simulation results with NS-2 in Section 5 shows that the obtained bounds estimate is still applicable when RTT is actually time-varying.

Notice that the AIMD/RED system defined by (1) and (2) are described by delayed differential equations. The initial conditions are given by $1 \leq W(t) \leq W^*$ and $0 \leq q(t) \leq q^*$ on the interval $t \in [-R, 0]$. According to (1), it is also reasonable that we let $\dot{W}(t) \leq \frac{\alpha}{R}$ for $t \in [-R, 0]$.

Theorem 1. Let $U_B > 0$ be the largest real root of

$$U_B \cdot (U_B - \alpha) \cdot \left(U_B - \frac{R \cdot C}{N} - \alpha \right)^2 = \frac{\alpha^2(1 + \beta)}{(1 - \beta)NK_p}, \quad (3)$$

then $W(t) \leq U_B$ for $t \geq 0$.

The proof can be found in Appendix A.

If all AIMD flows are TCP-friendly, i.e., the average throughput of non-TCP-transported flows over a large time scale equals that of any conformant TCP-transported ones under the same circumstance [16], the (α, β) pair should satisfy the TCP-friendly condition $\alpha = 3(1 - \beta)/(1 + \beta)$ derived in [19,20]. Thus, the above equality (3) becomes

$$U_B \cdot (U_B - \alpha) \cdot (U_B - R \cdot C/N - \alpha)^2 = \frac{3\alpha}{NK_p}. \quad (4)$$

By the continuity property of $U_B \cdot (U_B - \alpha) \cdot (U_B - R \cdot C/N - \alpha)^2$ and the fact that the RHS of (3) is always greater than zero, we can conclude that the largest root of (3) must be greater than $R \cdot C/N + \alpha$, where $R \cdot C/N$ is the equilibrium value of the window size for AIMD/RED system. Therefore, the oscillation of the window size from its equilibrium value will increase with the increment of α and the decrement of K_p .

3.3. Lower bound on window size and upper bound on queue length

In the previous subsection, we proved that the AIMD window size $W(t)$ is bounded from above, and an upper bound, U_B , is defined by (3). In this subsection, we show that the window size is also bounded from below while the queue length is upper bounded.

Theorem 2. Define $A := \frac{\alpha}{R} - \frac{2(1-\beta)U_B^2}{1+\beta R}$ and let $L_{B1} > 0$ be the root of

$$L_{B1} \cdot (L_{B1} - AR) = \frac{\alpha(1 + \beta)}{2(1 - \beta)},$$

then $W(t) \geq L_{B1}$ for $t \geq 0$.

The proof can be found in Appendix B.

Notice that L_{B1} in Theorem 2 is the lower bound of $W(t)$ for all $t \geq 0$, which is a global one. By similar analysis to the upper bound of window size U_B , it is easy to check that the window size $W(t)$ will not go below L_{B1} for any $t > t_2$. However, the value of L_{B1} is actually very small since $\alpha(1 + \beta)/(2(1 - \beta))$ is fairly small compared to $-AR$. Therefore, the global lower bound does not provide much information about the performance of AIMD/RED systems.

Since the window size oscillates around its equilibrium in the steady state, the amplitude of the oscillation is more important than the global lower bound. Next, we will show the local lower bound of the window size after the first time it reaches the peak value at moment t_1 . This local lower bound is more useful for understanding the performance of AIMD/RED systems.

Theorem 3. Define T_1 and U_Q as

$$T_1 = \frac{U_B - \frac{R \cdot C}{N}}{\frac{2(1-\beta)}{1+\beta} \cdot \frac{C \cdot K_p}{N} \cdot \left[\frac{R \cdot C}{N} \Delta q + \Delta W(q_0^* + \Delta q) \right]}$$

$$U_Q = \inf_{\substack{\Delta q > 0, \\ \Delta W \in [0, U_B - \frac{R \cdot C}{N}]}} \left\{ (q_0^* + \Delta q) + \left(\frac{N}{R} \cdot U_B - C \right) \cdot (T_1 + R) \right\},$$

where U_B is defined in Theorem 1. Let $L_{B2} > 0$ satisfy

$$L_{B2} \cdot \left(L_{B2} + \frac{2(1-\beta)}{1+\beta} U_B^2 \cdot K_p \cdot U_Q - \alpha \right) \cdot K_p \cdot U_Q = \frac{\alpha(1 + \beta)}{2(1 - \beta)},$$

then $q(t) \leq U_Q$ for $t \geq 0$ and $W(t) \geq L_{B2}$ for $t \geq t_1$.

The proof can be found in Appendix C.

Therefore, the homogeneous-flow AIMD/RED system is practically stable with the bounds derived in Theorems 1 and 3.

4. Bounds and practical stability of heterogeneous AIMD/RED systems with time delays

4.1. A fluid-flow model of Heterogeneous AIMD/RED system

In this section, we study the AIMD/RED system with heterogeneous flows, considering time delays. We here consider the case when there are two classes of flows with parameters (α_1, β_1) , (α_2, β_2) , time-invariant traffic loads N_1, N_2 , respectively, as depicted in Fig. 1. We assume that all the flows have the same round-trip time. The model in this section can be extended to any certain number of flows in multiple classes with heterogeneous AIMD parameters.

Taking time delays into consideration, a heterogeneous AIMD/RED system shared by two classes of flows can be modeled as

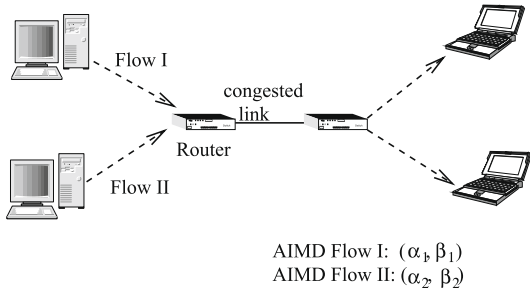


Fig. 1. Heterogeneous AIMD/RED system.

$$\begin{aligned} \frac{dW_I(t)}{dt} &= \frac{\alpha_1}{R(t)} - \frac{2(1-\beta_1)}{1+\beta_1} \frac{W_I(t)W_I(t-R(t))}{R(t-R(t))} K_p q(t-R(t)), \\ \frac{dW_{II}(t)}{dt} &= \frac{\alpha_2}{R(t)} - \frac{2(1-\beta_2)}{1+\beta_2} \frac{W_{II}(t)W_{II}(t-R(t))}{R(t-R(t))} K_p q(t-R(t)), \\ \frac{dq(t)}{dt} &= \begin{cases} \frac{N_1 W_I(t)}{R(t)} + \frac{N_2 W_{II}(t)}{R(t)} - C, & q > 0, \\ \left\{ \frac{N_1 W_I(t)}{R(t)} + \frac{N_2 W_{II}(t)}{R(t)} - C \right\}^+, & q = 0. \end{cases} \end{aligned} \quad (5)$$

Again, we simplify the above system by assuming $R(t) = R$. It is shown in [2] that $W_i(t)W_i(t-R)$ in (5) can be approximated by $W_i^2(t)$ for $i = I, II$ when the window size is much larger than one. We apply this approximation in the following analysis for the convenience of computation.

For the heterogeneous system (5), the equilibrium point (W_I^*, W_{II}^*, q_0^*) is given by

$$W_I^* = \frac{GCR}{N_1 G + N_2}, \quad W_{II}^* = \frac{CR}{N_1 G + N_2}, \quad q_0^* = \frac{\alpha_1(1+\beta_1)}{2(1-\beta_1)W_I^{*2}K_p},$$

where $G = \sqrt{\frac{\alpha_1(1+\beta_1)(1-\beta_2)}{\alpha_2(1-\beta_1)(1+\beta_2)}}$.

The physical significance of studying the stability properties of the equilibrium point of AIMD/RED system is because the equilibrium point is the most desired operating point of the system. At the equilibrium, the total window size is $N_1 W_I^* + N_2 W_{II}^*$ and the total arrival rate equals the total link capacity, thus the link bandwidth is fully utilized.

In (5), we take $\bar{W}(t) = N_1 \cdot W_I(t) + N_2 \cdot W_{II}(t)$, $M_1 = \frac{(1-\beta_1)}{1+\beta_1}$, $M_2 = \frac{(1-\beta_2)}{1+\beta_2}$, $r_1 = M_1/N_1$, and $r_2 = M_2/N_2$, then

$$\begin{aligned} \dot{\bar{W}} &= (N_1 \alpha_1 + N_2 \alpha_2)/R - 2[r_1 \cdot (N_1 W_I)^2(t) \\ &\quad + r_2 \cdot (N_2 W_{II})^2(t)] \cdot K_p q(t-R)/R. \end{aligned} \quad (6)$$

Note that $W_i(t) \geq 0$ for $i = I, II$. Taking $r_{\min} = \min(r_1, r_2)$, and $r_{\max} = \max(r_1, r_2)$, the following inequality can be obtained:

$$-2r_{\max} \frac{\bar{W}^2(t)}{R} \leq \frac{\dot{\bar{W}}(t) - \frac{N_1 \alpha_1 + N_2 \alpha_2}{R}}{K_p q(t-R)} \leq -r_{\min} \frac{\bar{W}^2(t)}{R}. \quad (7)$$

Also, we have

$$\dot{q}(t) = \begin{cases} \bar{W}(t)/R - C, & q > 0, \\ \{\bar{W}(t)/R - C\}^+, & q = 0. \end{cases} \quad (8)$$

Thus, with the new variable pair $(\bar{W}(t), q(t))$, the original heterogeneous AIMD/RED system (5) can be rewritten by (6) and (8). We will study the properties of $(\bar{W}(t), q(t))$

in the following to show the practical stability and derive the bounds of the system.

Remark 2. Our focus in the analysis below is $\bar{W}(t)$, the total window size at t . This is because $\bar{W}(t)$ indicates the entire throughput of the heterogeneous AIMD/RED system, which is more useful than the throughput of each individual flow.

4.2. Upper bound on window size

The bounds estimate of the heterogeneous AIMD/RED system are given in the following.

Theorem 4. Let $\bar{U}_B > 0$ be the largest real root of

$$\bar{U}_B^2 \cdot [\bar{U}_B - R \cdot C - (N_1 \alpha_1 + N_2 \alpha_2)]^2 = \frac{4(N_1 \alpha_1 + N_2 \alpha_2)^2}{r_{\min} \cdot K_p}, \quad (9)$$

then $\bar{W}(t) \leq \bar{U}_B$ for $t \geq 0$.

Proof. With (6), $\dot{\bar{W}}(t) \leq (N_1 \alpha_1 + N_2 \alpha_2)/R$ for $t \geq 0$. For $\tau > 0$, take integration on both sides from $t - \tau$ to t :

$$\bar{W}(t) - \bar{W}(t - \tau) \leq (N_1 \alpha_1 + N_2 \alpha_2) \cdot \tau / R. \quad (10)$$

We show that $\bar{U}_B > 0$ in the theorem is an upper bound of $\bar{W}(t)$ for $t \geq 0$, i.e., if $\bar{W}(t) = \bar{U}_B$ for some $t = \bar{t}_1 \geq 0$, then $\dot{\bar{W}}(\bar{t}_1) \leq 0$.

Integrating on both sides of (8) from $\bar{t}_1 - a \cdot R$ to $\bar{t}_1 - R$ for $a > 1$ gives

$$\int_{\bar{t}_1 - aR}^{\bar{t}_1 - R} \dot{q}(s) ds \geq \frac{1}{R} \int_{\bar{t}_1 - aR}^{\bar{t}_1 - R} \bar{W}(s) ds - (a-1)R \cdot C.$$

Note that (10) implies $\bar{W}(\bar{t}_1 - \tau) \geq \bar{U}_B - a \cdot (N_1 \alpha_1 + N_2 \alpha_2)$ when $\tau \in [R, aR]$. Thus,

$$q(\bar{t}_1 - R) \geq [\bar{U}_B - a \cdot (N_1 \alpha_1 + N_2 \alpha_2)] \cdot (a-1) - R \cdot C \cdot (a-1), \quad (11)$$

since $q(t) \geq 0$.

Taking $f(a) = (a-1) \cdot [\bar{U}_B - a \cdot (N_1 \alpha_1 + N_2 \alpha_2)] - R \cdot C$ and computing the maximum value of $f(a)$ by letting $f'(a) = 0$ gives

$$f(a) = [\bar{U}_B - R \cdot C - (N_1 \alpha_1 + N_2 \alpha_2)]^2 / [4(N_1 \alpha_1 + N_2 \alpha_2)], \quad (12)$$

with $a = [\bar{U}_B - R \cdot C + (N_1 \alpha_1 + N_2 \alpha_2)] / [2(N_1 \alpha_1 + N_2 \alpha_2)]$ and $f''(a) < 0$.

Therefore, it follows from (7), (11) and (12) that, $\dot{\bar{W}}(\bar{t}_1) \leq 0$ if \bar{U}_B satisfies

$$\bar{U}_B^2 \cdot [\bar{U}_B - R \cdot C - (N_1 \alpha_1 + N_2 \alpha_2)]^2 = \frac{4(N_1 \alpha_1 + N_2 \alpha_2)^2}{r_{\min} \cdot K_p}, \quad (13)$$

which implies $\bar{W}(t) \leq \bar{U}_B$ for $t \geq 0$.

It is also noted that the upper bound derived here is global for the time t , i.e., the window size $\bar{W}(t)$ will not go above \bar{U}_B for any $t > \bar{t}_1$. If we assume, instead, that there exists $\bar{t}'_1 > \bar{t}_1$ and $\Delta W > 0$, such that $\bar{W}(\bar{t}'_1) = \bar{U}_B + \Delta W$, there must be some $\tau' \in (0, \bar{t}'_1 - \bar{t}_1)$ such that $\bar{W}(\bar{t}'_1 - \tau') = \bar{U}_B$ and $\dot{\bar{W}}(\bar{t}'_1 - \tau') > 0$. However, similar to

the proof of Theorem 4, we have $\dot{\bar{W}}(\bar{t}_1 - \tau') \leq 0$, which is a contradiction. Therefore, the window size is upper bounded by \bar{U}_B for all $t \geq 0$. \square

By the continuity property of $\bar{U}_B^2 \cdot \bar{U}_B - R \cdot C - (N_1\alpha_1 + N_2\alpha_2)^2$ and the fact that the RHS of (9) is always greater than zero, we can conclude that there exists at least one real root for (9) and the largest root must be greater than $R \cdot C + (N_1\alpha_1 + N_2\alpha_2)$. Therefore, the upper bound \bar{U}_B itself will increase with the increment of $R \cdot C$ and $(N_1\alpha_1 + N_2\alpha_2)$. In addition, the oscillation of the window size from its equilibrium value will increase with the increment of $N_1\alpha_1 + N_2\alpha_2$ and the decrement of K_p .

4.3. Lower bound on window size and upper bound on queue length

In this subsection, we prove that the window size of heterogeneous-flow system is also lower bounded while the queue length is upper bounded.

Theorem 5. Let $\bar{L}_{B1} := \left(\frac{N_1\alpha_1 + N_2\alpha_2}{2 \cdot r_{\max}}\right)^{1/2}$, then $\bar{W}(t) \geq \bar{L}_{B1}$ for $t \geq 0$.

Proof. Showing that $\bar{L}_{B1} > 0$ is the lower bound of $\bar{W}(t)$ for $t \geq 0$, we should prove that if $\bar{W}(t) = \bar{L}_{B1}$ at time $t = \bar{t}_2 \geq 0$, then $\dot{\bar{W}}(\bar{t}_2) \geq 0$.

Since the dropping/marking probability $p(t) = K_p \cdot q \leq 1$ for all t , then

$$\begin{aligned} \dot{\bar{W}}(\bar{t}_2) &\geq \frac{N_1\alpha_1 + N_2\alpha_2}{R} - 2 \cdot r_{\max} \frac{\bar{W}^2(t)}{R} K_p q(t - R) \\ &\geq \frac{N_1\alpha_1 + N_2\alpha_2}{R} - 2 \cdot r_{\max} \frac{\bar{W}^2(t)}{R}. \end{aligned}$$

Therefore, $\dot{\bar{W}}(\bar{t}_2) \geq 0$ when $\bar{W}(t) = \bar{L}_{B1}$ with \bar{L}_{B1} defined in the theorem, which implies $\bar{W}(t) \geq \bar{L}_{B1}$ for $t \geq 0$.

Note that \bar{L}_{B1} in Theorem 5 is the lower bound of $\bar{W}(t)$ for all $t \geq 0$, which is a global bound. To show this, similar analysis to the upper bound of window size \bar{U}_B can be applied to check that the window size $\bar{W}(t)$ will not go below \bar{L}_{B1} for any $t > \bar{t}_2$. \square

The local lower bound of the window size after the first time it reaches the peak value at \bar{t}_1 is derived below.

Theorem 6. Define \bar{T}_1 and \bar{U}_Q as

$$\begin{aligned} \bar{T}_1 &:= \frac{\bar{U}_B - R \cdot C}{r_{\min} \cdot RC^2 \cdot K_p \cdot (q_0^* + \Delta q) - \frac{N_1\alpha_1 + N_2\alpha_2}{R}}, \\ \bar{U}_Q &:= \inf_{\Delta q > 0} \left\{ (q_0^* + \Delta q) + \left(\frac{\bar{U}_B}{R} - C\right) \cdot (\bar{T}_1 + R) \right\}, \end{aligned}$$

where \bar{U}_B is defined in Theorem 4. Let $\bar{L}_{B2} > 0$ satisfy

$$\bar{L}_{B2}^2 \cdot K_p \cdot \bar{U}_Q = \frac{N_1\alpha_1 + N_2\alpha_2}{2r_{\max}}, \quad (14)$$

then $q(t) \leq \bar{U}_Q$ for $t \geq 0$ and $\bar{W}(t) \geq \bar{L}_{B2}$ for $t \geq \bar{t}_1$.

Proof. We first derive the upper bound of $q(t)$ for $t \geq 0$. Suppose that $\bar{W}(t)$ reaches its peak value at moment $t = \bar{t}_1$. To get a loose upper bound of $q(t)$, we introduce the comparison theorem [26]. Instead of following system

(6) and (8), we consider its comparison system: $\dot{q}(t) = \bar{U}_B/R - C$, and $\bar{W}(t) \equiv \bar{U}_B$ for $t \in [\bar{t}_1, \bar{t}_1]$. Note that the solutions of the comparison system are larger than those of the original system, so the bounds derived in the following are also the bounds for system (6) and (8).

Assume that $\bar{W}(t)$ does not decrease for some time after \bar{t}_1 , and thus $q(t)$ increases at the rate of $\bar{U}_B/R - C$. \bar{t}_1 is chosen such that $q(\bar{t}_1) = q^* + \Delta q$ with $\Delta q > 0$, then $\bar{W}(t)$ decreases from \bar{t}_1 while $q(t)$ keeps increasing till \bar{t}_2 such that $\dot{q}(\bar{t}_2) = 0$ ($\bar{W}(\bar{t}_2) = RC$) with $\bar{t}_2 \geq \bar{t}_1 + R$. Therefore, $q(\bar{t}_2)$ is the local maximum value of $q(t)$. This estimate of $q(t)$ might be greater than the real maximum value of $q(t)$ since $\bar{W}(t)$ may not stay at its peak value after \bar{t}_1 , and $q(t)$ will still increase after \bar{t}_1 , but with the rate less than $\bar{U}_B/R - C$.

From the above analysis, for $t \in [\bar{t}_1, t_2]$, $\dot{q}(t) \leq \frac{\bar{U}_B}{R} - C$, which implies

$$\begin{aligned} q(\bar{t}_2) &\leq q(\bar{t}_1) + \left(\frac{\bar{U}_B}{R} - C\right) \cdot (\bar{t}_2 - \bar{t}_1) \\ &= (q_0^* + \Delta q) + \left(\frac{\bar{U}_B}{R} - C\right) \cdot (\bar{t}_2 - \bar{t}_1). \end{aligned} \quad (15)$$

To estimate the length of the interval $[\bar{t}_1, \bar{t}_2]$, for $t \in [\bar{t}_1 + R, \bar{t}_2]$, it follows from the analysis above that

$$\begin{aligned} \bar{W}(t) &\geq \bar{W}(\bar{t}_2) = RC, \\ q(t - R) &\geq q(\bar{t}_1) = q_0^* + \Delta q, \end{aligned}$$

for some $\Delta q > 0$.

Thus,

$$\dot{\bar{W}}(t) \leq \frac{N_1\alpha_1 + N_2\alpha_2}{R} - r_{\min} \cdot \frac{(RC)^2}{R} \cdot K_p \cdot (q_0^* + \Delta q), \quad (16)$$

for $t \in [\bar{t}_1 + R, \bar{t}_2]$.

On the other hand,

$$\int_{\bar{t}_1 + R}^{\bar{t}_2} \dot{\bar{W}}(s) ds = \bar{W}(\bar{t}_2) - \bar{W}(\bar{t}_1 + R) \geq RC - \bar{U}_B. \quad (17)$$

It follows from (16) and (17) that,

$$\begin{aligned} RC - \bar{U}_B &\leq \left[(N_1\alpha_1 + N_2\alpha_2)/R - r_{\min} \cdot RC^2 \cdot K_p \cdot (q_0^* + \Delta q) \right] \\ &\quad \cdot (\bar{t}_2 - \bar{t}_1 - R), \end{aligned}$$

i.e.,

$$\bar{t}_2 - \bar{t}_1 - R \leq \frac{\bar{U}_B - RC}{r_{\min} RC^2 K_p (q_0^* + \Delta q) - (N_1\alpha_1 + N_2\alpha_2)/R}.$$

With the definition of \bar{T}_1 in Theorem 6, we have $\bar{t}_2 - \bar{t}_1 \leq \bar{T}_1 + R$. Therefore, it follows from (15) that

$$q(t) \leq \inf_{\Delta q > 0} \left\{ (q_0^* + \Delta q) + \left(\frac{\bar{U}_B}{R} - C\right) \cdot (\bar{T}_1 + R) \right\}, \quad (18)$$

i.e., $q(t) \leq \bar{U}_Q$ for $t \geq 0$, which indicates that \bar{U}_Q is the upper bound of the RED queue length. Since the packet loss in a RED queue is proportional to the queue length, the derived queue length upper bound also reflects the maximum packet loss rate.

We finally show that $\bar{L}_{B2} > 0$ is a lower bound of $\bar{W}(t)$ for $t \geq \bar{t}_1$, i.e., if $\bar{W}(t) = \bar{L}_{B2}$ at time $t = \bar{t}_3 > \bar{t}_1$, then $\dot{\bar{W}}(\bar{t}_3) \geq 0$.

With (7) and (18),

$$\dot{\bar{W}}(\bar{t}_3) \geq \frac{N_1 \alpha_1 + N_2 \alpha_2}{R} - 2r_{\max} \cdot \frac{\bar{L}_{B2}^2}{R} \cdot K_p \cdot \bar{U}_Q.$$

Thus, $\dot{\bar{W}}(\bar{t}_3) \geq 0$ if \bar{L}_{B2} is chosen to satisfy (14).

Therefore, \bar{L}_{B2} is the lower bound of $\bar{W}(t)$ for $t \geq \bar{t}_1$. \square

Therefore, the heterogeneous AIMD/RED system is practically stable with the bounds derived in Theorems 4 and 6.

Remark 3. The approach applied in this section can also be extended to obtain the theoretical bounds for the AIMD/RED system when it is shared by more than two classes of flows. Details are omitted here due to space limit.

5. Performance evaluation

In this section, we first use Matlab to simulate the AIMD/RED system described by the fluid-flow model to get the maximum and minimum window size and queue length, and compare them with the derived bounds. We then use NS-2 [27] to simulate a more realistic AIMD/RED system to validate the bounds. How the system performance is affected by different parameters is also evaluated by the simulations.

5.1. Verify the bounds of the fluid-flow model using Matlab simulations

5.1.1. AIMD parameter pair

First, we investigate how the AIMD parameter pair (α, β) affects the bounds. Let N, R, C and K_p be constants: $N = 10, R = 0.1$ s, $C = 1000$ packet/s and $K_p = 0.01$. The

Table 1
Bounds with different (α, β) .

(α, β)	W_{\max}	U_B	W_{\min}	L_{B2}	Q_{\max}	U_Q
(9/5, 1/4)	12.22	12.44	1.06	0.06	24.70	39.20
(1, 1/2)	11.33	11.50	3.32	0.26	17.30	26.50
(3/7, 3/4)	10.65	10.76	6.87	1.28	10.95	17.70
(1/5, 7/8)	10.36	10.43	8.68	2.90	7.70	12.80
(3/31, 15/16)	10.21	10.26	9.42	3.58	5.88	10.10

Table 2
AIMD/RED system bounds with $(\alpha, \beta) = (1, 1/2)$.

#	N	R	C	K_p	(W^*, q^*)	W_{\max}	U_B	W_{\min}	L_{B2}	Q_{\max}	U_Q
1	10	0.02	1e3	1e-2	(2, 37.5)	4.04	4.41	1.52	0.09	51	147.5
2	10	0.05	1e3	1e-2	(5, 6)	6.60	6.80	2.13	0.32	28	43.3
3	20	0.05	2e3	5e-3	(5, 12)	6.60	6.80	2.12	0.38	56	78
4	10	0.05	1e3	5e-3	(5, 12)	6.82	7.10	2.78	0.66	39	54.6
5	10	0.4	1e3	5e-3	(40, 3/16)	41.30	42.02	14.14	0.11	10	23.2
6	10	0.05	1e4	5e-3	(50, 3/25)	51.09	51.15	23.22	0.18	8	14.1
7	20	0.05	2e4	5e-3	(50, 3/25)	51.00	51.20	8.91	0.068	15	23.1
8	1e2	0.05	1e4	5e-3	(5, 12)	6.28	6.41	0.72	0.04	153	241.6
9	1e3	0.1	1e6	1e-3	(100, 3/20)	101.0	101.02	3e-2	2e-4	577	1024
10	1e4	0.1	1e6	1e-3	(10, 15)	11.04	11.05	2e-2	2e-4	6731	10785
11	1e4	0.1	1e6	5e-3	(10, 3)	11.017	11.023	5e-3	7e-6	5942	10349
12	1e4	0.1	1e6	1e-2	(10, 3/2)	11.011	11.016	2e-3	2e-6	5714	10248

AIMD (α, β) pairs are chosen to be TCP-friendly, varying from (9/5, 1/4) to (3/31, 15/16). The derived bounds and the numerical results with Matlab are given in Table 1. It can be seen that for the window size and the queue length, the numerical results (W_{\max} , W_{\min} , and Q_{\max}) are all within the bounds (U_B , L_{B2} , and U_Q) given by Theorems 1 and 3, which verifies the correctness of the Theorems. In addition, the derived upper bound of the window size is very tight. The one for queue length is a loose bound as mentioned in the proof of Theorem 3. The theoretical lower bound of window size is also loose because of the approximation of $\dot{W}(t)$ in (C.5). How to find a tight lower bound for window size requires further research.

Another observation is that the difference between the numerical results and the derived bounds is getting smaller as (α, β) pair varies from (9/5, 1/4) to (3/31, 15/16), which shows that the derived bounds become tighter when the value of β gets larger.

In ideal cases, the window size should converge to $R \cdot C/N$, which is 10 packets per RTT in the above cases. The results in Table 1 show that with a smaller value of α and a larger value of β , the AIMD flows have less oscillation amplitude around the optimal operation point, so they can utilize network resources more efficiently with less delay and loss in steady state. This is because, with a smaller value of α , the AIMD flows overshoot the available bandwidth in a slower pace; with a larger value of β , the AIMD flows will not decrease drastically for any single packet loss. Also, as shown in Table 1, the upper bound of the queue length becomes smaller w.r.t. β ; thus, the average queueing delay (and thus loss rate) becomes smaller in steady state.

5.1.2. Round-trip delay and link capacity

In the following, we study how the system parameters N, R, C and K_p affect the bounds. We choose (α, β) pair to be (1, 1/2) and (1/5, 7/8), and obtain the results with different network parameters as shown in Tables 2 and 3, respectively.

First, compare rows 1 and 2 in Tables 2 and 3. By enlarging the delay from 0.02 s to 0.05 s (by 2.5 times), the upper bound of window sizes only increases by 1.54 times and 1.86 times for TCP and AIMD (1/5, 7/8), respectively, which means a larger delay reduces the relative oscillation amplitude of window size. In addition, the upper bound of

Table 3AIMD/RED system bounds with $(\alpha, \beta) = (1/5, 7/8)$.

#	N	R	C	K_p	(W^*, q^*)	W_{\max}	U_B	W_{\min}	L_{B2}	Q_{\max}	U_Q
1	10	0.02	1e3	1e-2	(2, 37.5)	2.81	3.03	1.76	0.59	55.39	135.5
2	10	0.05	1e3	1e-2	(5, 6)	5.50	5.63	4.19	1.77	17.64	31.20
3	20	0.05	2e3	5e-3	(5, 12)	5.51	5.65	4.19	1.65	35.3	65.2
4	10	0.05	1e3	5e-3	(5, 12)	5.62	5.80	4.27	2.10	29.13	48.70
5	10	0.4	1e3	5e-3	(40, 3/16)	40.25	40.29	36.79	5.38	3.10	5.21
6	10	0.05	1e4	5e-3	(50, 3/25)	50.23	50.26	45.93	6.31	2.48	3.85
7	20	0.05	2e4	5e-3	(50, 3/25)	50.23	50.26	43.99	3.24	4.28	7.10
8	1e2	0.05	1e4	5e-3	(5, 12)	5.34	5.46	3.76	1.39	67	84
9	1e3	0.1	1e6	1e-3	(100, 3/20)	100.20	100.21	39.26	0.025	127	211
10	1e4	0.1	1e6	1e-3	(10, 15)	10.22	10.23	2.02	0.02	1667	2361
11	1e4	0.1	1e6	5e-3	(10, 3)	10.208	10.211	0.07	9.7e-4	1355	2159
12	1e4	0.1	1e6	1e-2	(10, 3/2)	10.205	10.207	0.015	2.4e-4	1266	2112

queue length decreases. Similar trend can be found if comparing rows 4 and 5 in both tables. This is a surprising result. From [3], a longer delay may drive the system from stable to unstable. We can explain it as follows. A larger delay means that the window size increasing speed (in terms of packet per second) during the additive increase period is smaller, and the AIMD flows will overshoot the network capacity in a slower pace (similar to the effect of a smaller value of α); thus, the upper bound of window size is closer to the optimal operating point, and the maximum queue length is smaller.

Another surprising result is found if we compare rows 4 and 6 in both tables. By enlarging the link capacity by 10 times, the upper bound of window size is increased by 7.5 and 8.9 times, for TCP and AIMD (1/5, 7/8), respectively. Although enlarging the link capacity may drive the system from stable to unstable [3], the oscillation amplitude of window size (relative to the equilibrium W^*) and queue length will actually decrease. Simulation results with NS-2 also demonstrate the same tendency, as shown in Fig. 2 in Section 5.3.

5.1.3. Number of flows

Comparing rows 3 and 4, or rows 6 and 7 in Tables 2 and 3, we conclude that if we increase the number of flows and the link capacity proportionally, the bounds of window size are almost un-affected. With twice the flows multiplexed in a twice capacity link, the upper bound of queue length increases less than twice. Therefore, the queuing delay bound is slightly reduced because of the multiplexing gain.

Comparing rows 6 and 8 in Tables 2 and 3, if we increase the number of flows in the same link, the NU_B becomes larger. In other words, the oscillation of window size will increase significantly if the number of flows in a link increases, and the queuing delay will also increase significantly. This can be understood as N AIMD (α, β) flows will increase their windows by $N\alpha$ packets per RTT, and the larger the increasing rate during the Additive Increase stage, the more significantly the flows will overshoot the link capacity. This suggests that we may limit the number of TCP/AIMD connections in a highly-multiplexed link or promote to use more conservative AIMD parameter pairs

to ensure that the queuing delay (and also the loss rate) is less than certain threshold.

5.1.4. K_p

Comparing rows 2 and 4 in Tables 2 and 3, with a smaller value of K_p , the bounds of both window size and queue length are larger.

5.1.5. High capacity delay link

The last four rows of Tables 2 and 3 are the upper bounds of the TCP/AIMD window size and queuing delay in a highly-multiplexed, high bandwidth (tens of Gbps), and long delay (0.1 s RTT) link. It can be seen that, for TCP flows, the queuing delay can be bounded to 10.785 ms if the K_p is chosen to be 0.001. The delay bound can be slightly reduced to 10.349 ms and 10.248 ms if K_p is increased to 0.005 and 0.01, respectively. The results show that although K_p can be adjusted to control the queuing delay in system, the impact is limited for high bandwidth cases.

On the other hand, limiting the number of flows or using more conservative AIMD pairs are more effective in reducing queuing delay. For instance, if the number of flows is reduced to 100 or 1000, the queuing delay bound can be reduced to 0.241 ms or 1.079 ms, respectively. If using an AIMD parameter pair of (1/5, 7/8), the queuing delay for 10,000 flows with $K_p = 0.001$ can be bounded to 2.361 ms only.

5.2. NS-2 simulations with homogeneous flows

In the following, we conduct extensive NS-2 simulations with more realistic TCP and AIMD protocols and network settings to verify the bounds derived. In the simulation, TCP and AIMD agents use TCP SACK congestion control. All senders are saturated, i.e., they always have data to send. All flows share the same bottleneck link. To eliminate the phase effect, the access links have slightly different propagation delays.

Fig. 2 shows the traces of TCP flows with AIMD parameter pair of (1, 1/2) and those of AIMD (1/5, 7/8) flows. Here, $N = 10, R = 0.05$ s and $K_p = 0.005$. $C = 1000$ packet/s in Fig. 2a and $C = 10,000$ packet/s in Fig. 2b and c. For NS-2 simulations, we set Q_{\min} of the RED queue to be 20 packets.

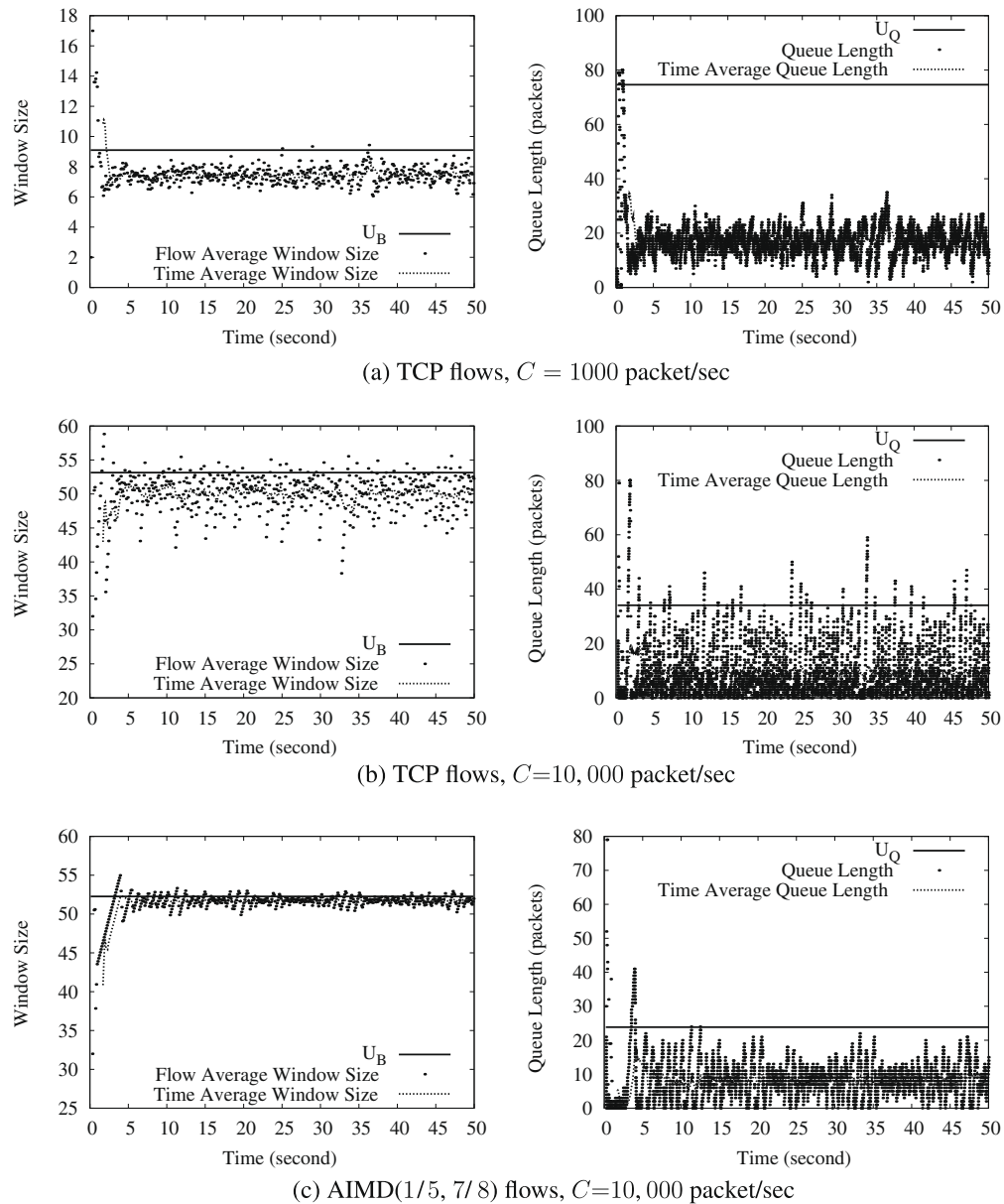


Fig. 2. Traces of flows window size and queue length, $N = 10$, $C = 10,000$ packet/s, $R = 0.05$ s and $K_p = 0.005$.

Therefore, the upper bound of each flow's window size should be enlarged by $Q_{\min}/N = 2$ packets, and the upper bound of the queue length should be enlarged by $Q_{\min} = 20$ packets. We compare the theoretical bounds with both the average window size among all flows and its time average over a round.

Simulation results demonstrate the tightness of the upper bound of window size. Also, although the window variation of AIMD (1/5, 7/8) in steady state is smaller, it takes longer time for AIMD (1/5, 7/8) flows to converge to the steady state. Another interesting observation is that although the upper bound of queue length is not tight comparing to the time average of queue length, it is close to the maximum instantaneous queue length in steady state.

5.3. NS-2 simulations with heterogeneous flows

Considering that the Internet might contain mixed traffic with different AIMD parameters, we further study the performance of the AIMD/RED system with heterogeneous flows. Parameters are firstly chosen as $C = 10,000$ packet/s, $K_p = 0.005$, and $R = 0.05$ s for 5 TCP flows competing with 5 AIMD (1/5, 7/8) flows. For comparison, we also choose $C = 20,000$ packet/s, $K_p = 0.005$, and $R = 0.05$ s for 10 TCP flows competing with 10 AIMD (1/5, 7/8) flows.

For the case of 5 TCP flows competing with 5 AIMD (1/5, 7/8) flows, the upper bound of $N_1 W_I + N_2 W_{II}$ is 508.9 packets, the lower bound \bar{L}_{B2} is 28.28 packets, and the upper bound of the queue length is 10.2 packets. For the case of 10 TCP flows competing with 10 AIMD (1/5, 7/8)

flows, the upper bound of $N_1W_I + N_2W_{II}$ is 1016.1 packets, the lower bound \bar{L}_{B2} is 55.80 packets, and the upper bound of queue length is 19.6 packets. In the NS-2 simulations, since the RED threshold \min_{th} is set to 20 packets, the upper bounds of total window size and queue length are enlarged by 20 packets accordingly. The correctness of our theoretical bounds and the tightness of the upper bound of window size are demonstrated by the simulation results, as shown in Fig. 3.

Similar to the observation with homogeneous flows, as shown in Fig. 3, if the number of flows and the link capacity are increased proportionally, the upper bound of per-flow window size is closer to its optimal value, and the upper bound of the queue length over link capacity is reduced. Therefore, the queuing delay bound is slightly reduced because of the multiplexing gain.

Fig. 4 shows the window trace and queue length when 20 TCP flows share the bottleneck with 40 AIMD (1/5, 7/8) flows with $K_p = 0.005$ and $K_p = 0.001$, respectively. For the case of $K_p = 0.005$, the upper bound of $N_1W_I + N_2W_{II}$ is 3034.4 packets and the upper bounds of queue length is 43.1 packets; while for the case of $K_p = 0.001$, the upper bound of total window size is 3042.4 packets and the upper bound of the queue length is 60.7 packets. It can be seen that a smaller value of K_p results in a slightly larger bounds on both window size and queue length. However, in the case of higher bandwidth, the impact of K_p is less significant.

In summary, our main findings are: (1) larger values of round-trip delay and link capacity will actually *reduce* the oscillation amplitude of the system and thus reduce the maximum queueing delay; (2) if we proportionally increase the link capacity and the number of AIMD flows, the queueing delay will be slightly reduced, thanks to the multiplexing gain; and (3) although TCP/AIMD flows can adapt their sending rates according to available bandwidth, larger number of flows leads to longer queueing delay in the AIMD/RED system, so admission control might be useful for future highly-multiplexed links.

6. Conclusion

In this paper, we have studied the practical stability of the AIMD/RED system by deriving theoretical bounds of window size and queue length of the AIMD/RED system for both homogeneous and heterogeneous flows cases. The theoretical results can provide important insights and guidelines for setting up parameters for the AIMD/RED system in order to maintain network stability and to fully utilize network resources without excessive delay and loss. The simulation results given in the paper can also help to predict and control the system performance for the next generation Internet with higher data rate links multiplexed with more flows with different parameters. The

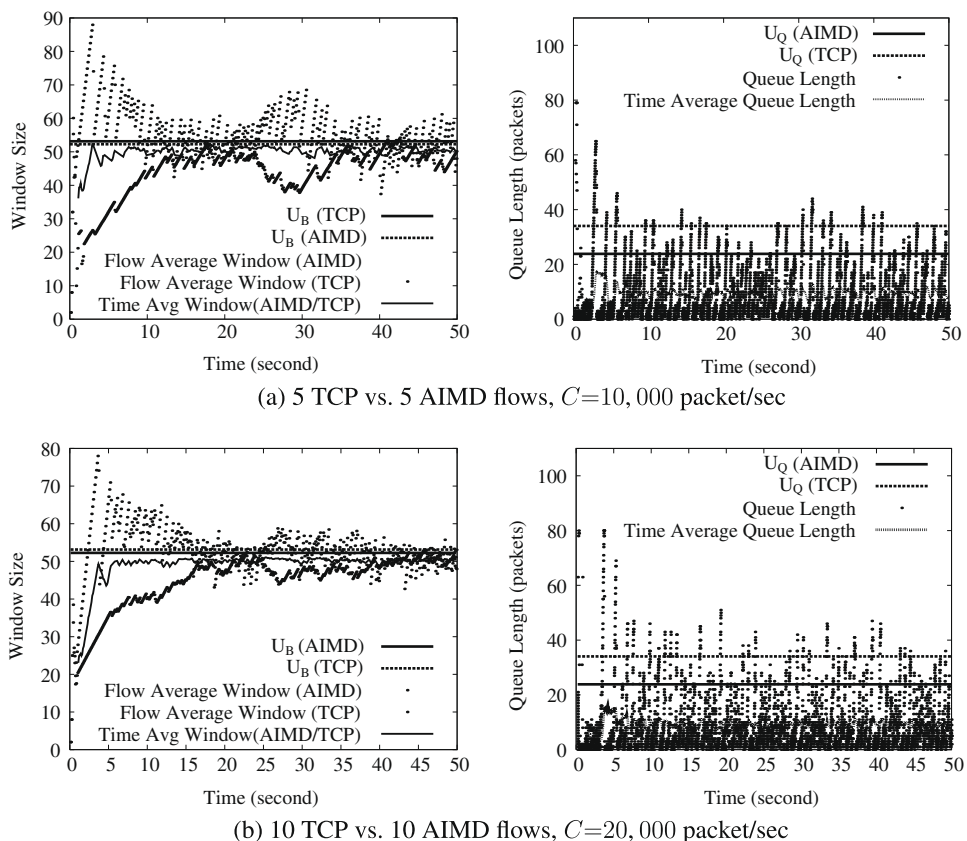


Fig. 3. Theoretical bounds of heterogeneous flows, $K_p = 0.005$, and $R = 0.05$ s.

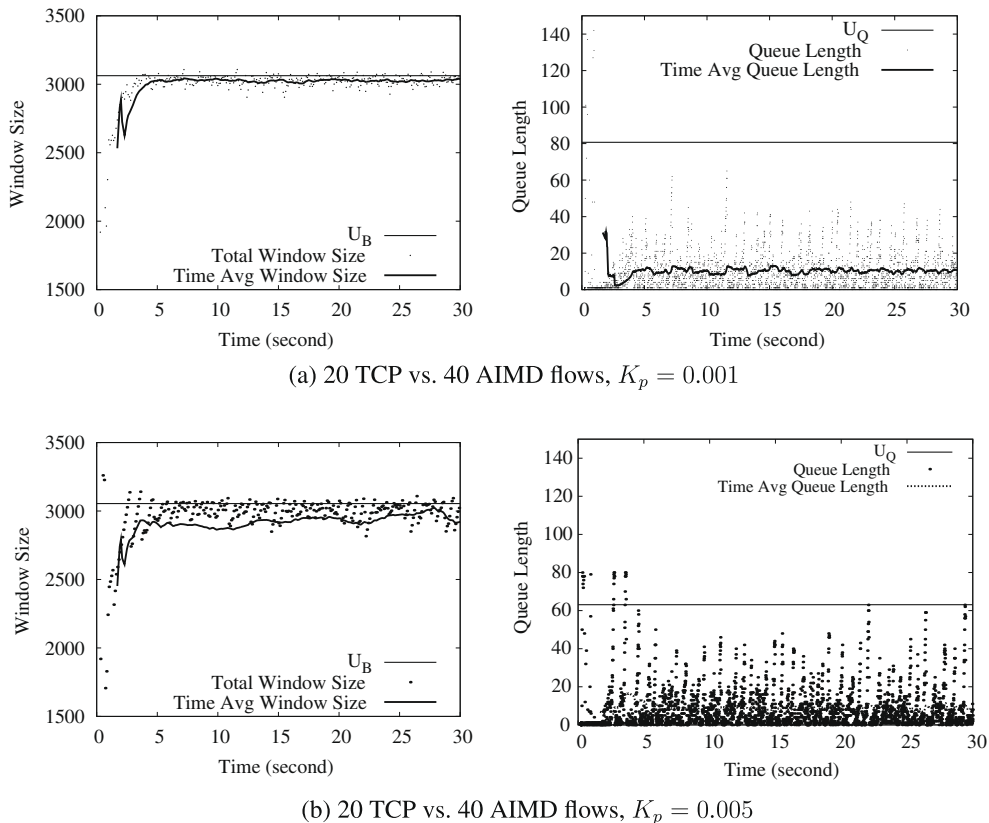


Fig. 4. Theoretical bounds of heterogeneous flows, $C = 60,000$ packet/s, and $R = 0.05$ s.

fluid-flow model analysis can also be applied to TCP-friendly rate control protocols.

There are many interesting research issues worth further investigation: (a) how to deploy effective admission control for TCP and AIMD flows to bound delay and loss; (b) how to adapt AIMD parameter pair to ensure that the system can converge to the equilibrium quick enough and to control the queuing delay and loss in the network; (c) how to extend the work to heterogeneous flows with different RTTs and multiple bottleneck links cases; and (d) how to consider the impact of short-lived flows on the bounds. On the other hand, with the popularity of wireless access technologies, it beckons for further research efforts to determine practical bounds in the wireless domain, considering the wireless channel characteristics and user mobility.

Acknowledgements

This work has been supported in part by research grants from the Natural Science and Engineering Council of Canada. The authors would like to thank the anonymous reviewers for their constructive comments.

Appendix A. Proof of Theorem 1

With (1) and (2), we note that $\dot{W} \leq \frac{\alpha}{R}$ for $t \geq 0$, since $W(t) \geq 1$ and $q(t) \geq 0$. For $\tau > 0$, taking integration on both sides from $t - \tau$ to t gives

$$W(t) - W(t - \tau) \leq \frac{\alpha}{R} \cdot \tau \quad \text{for } t \geq 0. \quad (\text{A.1})$$

We show that the U_B (> 0) in the theorem is an upper bound of $W(t)$ for $t \geq 0$, i.e., if $W(t) = U_B$ for some $t = t_1 \geq 0$, then $\dot{W}(t_1) \leq 0$.

With (A.1) and $W(t_1) = U_B$, and taking $\tau = R$ and $t = t_1$, we have

$$W(t_1 - R) \geq U_B - \alpha. \quad (\text{A.2})$$

Notice that $W(t_1 - \tau) \geq U_B - a \cdot \alpha$ when $\tau \in [R, aR]$ for any real number $a > 1$.

Consider

$$\dot{q}(t) = \begin{cases} \frac{N \cdot W(t)}{R} - C, & q > 0, \\ \left\{ \frac{N \cdot W(t)}{R} - C \right\}^+, & q = 0. \end{cases}$$

Taking integration on both sides from $t_1 - aR$ to $t_1 - R$, we have

$$\begin{aligned} \int_{t_1 - aR}^{t_1 - R} \dot{q}(s) ds &\geq \frac{N}{R} \int_{t_1 - aR}^{t_1 - R} W(s) ds - (a - 1)R \cdot C \\ &\geq N \cdot (a - 1) \cdot (U_B - a \cdot \alpha) - (a - 1)RC, \end{aligned}$$

which implies

$$q(t_1 - R) \geq [N \cdot (U_B - a \cdot \alpha) - R \cdot C] \cdot (a - 1), \quad (\text{A.3})$$

since $q(t) \geq 0$.

Taking $f(a) = (a - 1) \cdot [N \cdot (U_B - a \cdot \alpha) - R \cdot C]$ and computing the maximum value of $f(a)$ by letting $f'(a) = 0$ gives $a = (N \cdot U_B + R \cdot C + N \cdot \alpha) / (2\alpha N)$ and

$$f(a) = N(U_B - R \cdot C/N - \alpha)^2 / (2\alpha). \quad (\text{A.4})$$

Therefore, it follows from (A.2), (A.3) and (A.4) that, $\dot{W}(t_1) \leq 0$ since U_B satisfies

$$\frac{N \cdot U_B \cdot (U_B - \alpha) \cdot (U_B - R \cdot C/N - \alpha)^2}{2\alpha} = \frac{\alpha(1 + \beta)}{2(1 - \beta)K_p}, \quad (\text{A.5})$$

which implies $W(t) \leq U_B$ for $t \geq 0$.

It is also noted that the upper bound derived in Theorem 1 is a global one for the time t , i.e., the window size $W(t)$ will not go above U_B for any $t > t_1$. If we assume, instead, that there exists $t'_1 > t_1$ and $\Delta W > 0$, such that $W(t'_1) = U_B + \Delta W$, then there must be some $\tau \in (0, t'_1 - t_1)$ such that $W(t'_1 - \tau) = U_B$ and $\dot{W}(t'_1 - \tau) > 0$. However, similar to the proof of Theorem 1, we have $\dot{W}(t'_1 - \tau) \leq 0$, which is a contradiction. Therefore, the window size is upper bounded by U_B for any $t \geq 0$. \square

Appendix B. Proof of Theorem 2

Proof. From Theorem 1, $W(t) \leq U_B$ for $t \geq 0$, which implies

$$\dot{W}(t) \geq \frac{\alpha}{R} - \frac{2(1 - \beta)}{1 + \beta} \frac{U_B^2}{R} =: A.$$

It can be seen from the definition of U_B that $A < 0$. We show that $L_{B1} > 0$ is the lower bound of $W(t)$ for $t \geq 0$, i.e., if $W(t) = L_{B1}$ at time $t = t_2 \geq 0$, then $\dot{W}(t_2) \geq 0$.

Taking integration on both sides from $t_2 - R$ to t_2 gives $W(t_2 - R) \leq W(t_2) - AR = L_{B1} - AR$.

Since dropping/marking probability $p(t) = K_p \cdot q(t) \leq 1$ for all t , then $\dot{W}(t_2) \geq \frac{\alpha}{R} - \frac{2(1 - \beta)}{1 + \beta} \frac{L_{B1} \cdot (L_{B1} - AR)}{R}$. Therefore, $\dot{W}(t_2) \geq 0$ since L_{B1} satisfies

$$L_{B1} \cdot (L_{B1} - AR) = \frac{\alpha(1 + \beta)}{2(1 - \beta)}, \quad (\text{B.1})$$

which implies $W(t) \geq L_{B1}$ for $t \geq 0$. \square

Appendix C. Proof of Theorem 3

Proof. We first derive the upper bound of $q(t)$ for $t \geq 0$. At moment $t = t_1$, $W(t)$ reaches its peak value. To get a loose upper bound of $q(t)$, we introduce the comparison theorem [26]. Instead of following system (1), we consider its comparison system: $\dot{q}(t) = U_B/R - C$, and $W(t) \equiv U_B$ for $t \in [t_1, t'_1]$. Notice that the solutions of the comparison system are larger than those of the original system, so the bounds derived in the following are also the bounds for system (1).

Assume that $W(t)$ does not decrease for some time after t_1 , and thus $q(t)$ increases at the rate $\frac{N}{R}U_B - C$. Moment t'_1 is chosen such that $q(t'_1) = q^* + \Delta q$ with $\Delta q > 0$, then $W(t)$ decreases from t'_1 while $q(t)$ keeps increasing till moment

t_2 such that $\dot{q}(t_2) = 0$ (i.e., $W(t_2) = R \cdot C/N$). Therefore, $q(t_2)$ is the local maximum value of $q(t)$. It should be noticed that this estimate of $q(t)$ might be greater than the real maximum value of $q(t)$ since $W(t)$ may not stay at its peak value after t_1 , and $q(t)$ will still increase after t_1 , but with the rate less than $\frac{N}{R}U_B - C$.

From above analysis, for $t \in [t'_1, t_2]$, $\dot{q}(t) \leq \frac{N}{R} \cdot U_B - C$. Thus,

$$\int_{t'_1}^{t_2} \dot{q}(s) ds \leq \left(\frac{N}{R} \cdot U_B - C \right) \cdot (t_2 - t'_1),$$

which implies,

$$\begin{aligned} q(t_2) &\leq q(t'_1) + \left(\frac{N}{R} \cdot U_B - C \right) \cdot (t_2 - t'_1) \\ &= (q_0^* + \Delta q) + \left(\frac{N}{R} \cdot U_B - C \right) \cdot (t_2 - t'_1). \end{aligned} \quad (\text{C.1})$$

To estimate the length of the interval $[t'_1, t_2]$, for $t \in [t'_1 + R, t_2]$, it follows from the analysis above that

$$W(t) \geq W(t_2) = \frac{R \cdot C}{N},$$

$$q(t - R) \geq q(t'_1) = q_0^* + \Delta q,$$

$$W(t - R) \geq W(t_2 - R) = \frac{R \cdot C}{N} + \Delta W,$$

for some $\Delta q > 0$ and $\Delta W \in (0, U_B - \frac{R \cdot C}{N})$.

Thus,

$$\dot{W}(t) \leq -\frac{2(1 - \beta)}{1 + \beta} \cdot \frac{C \cdot K_p}{N} \cdot \left[\Delta W(q_0^* + \Delta q) + \frac{R \cdot C}{N} \Delta q \right], \quad (\text{C.2})$$

for $t \in [t'_1 + R, t_2]$.

On the other hand,

$$\int_{t'_1 + R}^{t_2} \dot{W}(s) ds = W(t_2) - W(t'_1 + R) \geq \frac{R \cdot C}{N} - U_B. \quad (\text{C.3})$$

It follows from (C.2) and (C.3) that,

$$\begin{aligned} \frac{R \cdot C}{N} - U_B &\leq -\frac{2(1 - \beta)}{1 + \beta} \cdot \frac{C \cdot K_p}{N} \cdot (t_2 - t'_1 - R) \\ &\quad \cdot \left[\Delta W(q_0^* + \Delta q) + \frac{R \cdot C}{N} \Delta q \right], \end{aligned}$$

i.e.,

$$t_2 - t'_1 - R \leq \frac{U_B - \frac{R \cdot C}{N}}{\frac{2(1 - \beta)}{1 + \beta} \cdot \frac{C \cdot K_p}{N} \cdot \left[\frac{R \cdot C}{N} \Delta q + \Delta W(q_0^* + \Delta q) \right]}.$$

With the definition of T_1 in the theorem, we have $t_2 - t'_1 \leq T_1 + R$. Therefore, it follows from (C.1) that

$$q(t) \leq \inf_{\substack{\Delta q > 0, \\ \Delta W \in [0, U_B - \frac{R \cdot C}{N}]}} \left\{ (q_0^* + \Delta q) + \left(\frac{N}{R} \cdot U_B - C \right) \cdot (T_1 + R) \right\}, \quad (\text{C.4})$$

i.e., $q(t) \leq U_Q$ for $t \geq 0$, which indicates that U_Q is the upper bound of the RED queue length. Since the packet loss in a RED queue is proportional to the queue length, the derived queue length upper bound also reflects the upper bound of packet loss rate.

We finally show that $L_{B2} > 0$ is a lower bound of $W(t)$ for $t \geq t_1$, i.e., if $W(t) = L_{B2}$ at time $t = t_3 > t_1$, then $\dot{W}(t_3) \geq 0$.

With (A.5) and (C.4),

$$\dot{W}(t) \geq \frac{\alpha}{R} - \frac{2(1-\beta)}{1+\beta} \cdot \frac{U_B^2}{R} \cdot K_p \cdot U_Q, \quad (C.5)$$

for $t \geq 0$, we have

$$\int_{t_3-R}^{t_3} \dot{W}(s) ds \geq \alpha - \frac{2(1-\beta)}{1+\beta} \cdot U_B^2 \cdot K_p \cdot U_Q,$$

i.e.,

$$W(t_3 - R) \leq L_{B2} + \frac{2(1-\beta)}{1+\beta} \cdot U_B^2 \cdot K_p \cdot U_Q - \alpha. \quad (C.6)$$

It follows from (C.4) and (C.6) that,

$$\dot{W}(t_3) \geq \frac{\alpha}{R} - \frac{2(1-\beta)}{1+\beta} \cdot \frac{L_{B2} \cdot U_W}{R} \cdot K_p \cdot U_Q,$$

with $U_W := L_{B2} + \frac{2(1-\beta)}{1+\beta} \cdot U_B^2 \cdot K_p \cdot U_Q - \alpha$.

Thus, $\dot{W}(t_3) \geq 0$ if L_{B2} is chosen to satisfy

$$L_{B2} \cdot U_W \cdot K_p \cdot U_Q = \frac{\alpha(1+\beta)}{2(1-\beta)}, \quad (C.7)$$

and thus L_{B2} is the lower bound of $W(t)$ for $t \geq t_1$. \square

References

- [1] R. Johari, D.K.H. Tan, End-to-end congestion control for the internet: delays and stability, *IEEE/ACM Transactions on Networking* 9 (6) (2001) 818–832.
- [2] C.V. Hollot, Y. Chait, Nonlinear stability analysis of a class of TCP/AQM networks, in: *Proceedings of the IEEE Conference on Decision and Control*, vol. 3, Orlando, Florida USA, Dec. 2001, pp. 2309–2314.
- [3] S. Low, F. Paganini, J. Wang, S. Adlakha, J.C. Doyle, Dynamics of TCP/RED and a scalable control, in: *IEEE Infocom'02*, vol. 1, Jun. 2002, pp. 239–248.
- [4] C.V. Hollot, V. Misra, D. Towsley, W.B. Gong, Analysis and design of controllers for AQM routers supporting TCP flows, *IEEE Transactions on Automatic Control* 47 (6) (2002) 945–959.
- [5] V. Firoiu, M. Borden, A study of active queue management for congestion control, in: *Proceedings of the IEEE Infocom*, 2000.
- [6] S. Floyd, V. Jacobson, Random early detection gateways for congestion avoidance, *IEEE/ACM Transactions on Networking* 1 (1997).
- [7] D. Lin, R. Morris, Dynamics of random early detection, in: *Proceedings of the ACM/SIGCOMM*, 1997.
- [8] Configuring weighted random early detection, Cisco IOS Release 12.0 Quality of Service Solutions Configuration Guide. <<http://www.cisco.com/>>, <en/US/docs/ios/12_0/qos/configuration/guide/qcwrred.pdf>.
- [9] Configuring dropping behavior with RED and WRED, Juniper quality of service configuration guide. <<http://www.juniper.net/techpubs/software/>>, <erx/junos90/swconfig-qos/html/drop-profiles-config.html>.
- [10] S. Shakkottai, R. Srikant, S. Meyn, Bounds on the throughput of congestion controllers in the presence of feedback delay, *IEEE Transactions on Networking* 11 (6) (2003) 972–981.
- [11] Z. Wang, F. Paganini, Boundedness and global stability of a nonlinear congestion control with delays, *IEEE Transactions on Automatic Control* 51 (9) (2006) 1514–1519.
- [12] L. Ying, G.E. Dullerud, R. Srikant, Global stability of internet congestion controllers with heterogeneous delays, *IEEE Transactions on Networking* 14 (3) (2006) 579–591.
- [13] S. Deb, R. Srikant, Global stability of congestion controllers for the internet, *IEEE Transactions on Automatic Control* 48 (6) (2003) 1055–1060.

- [14] S. Shakkottai, R. Srikant, How good are deterministic fluid model of internet congestion control? in: *IEEE Infocom'02*, vol. 2, Jul. 2002, pp. 497–505.
- [15] V. Misra, W.B. Gong, D. Towsley, Fluid-based analysis of a network of AQM routers supporting TCP flows, in: *Proceedings of the ACM/SIGCOMM*, 2000, pp. 151–160.
- [16] S. Floyd, K. Fall, Promoting the use of end-to-end congestion control in the internet, in: *IEEE/ACM Transactions on Networking*, vol. 7, no. 4, Aug. 1999, pp. 458–472.
- [17] S. Floyd, M. Handley, J. Padhye, A comparison of equation-based and AIMD congestion control, May 2000. <<http://www.aciri.org/tfrc/tcp-friendly.TR.ps>>.
- [18] Y.R. Yang, S.S. Lam, General AIMD congestion control, Technical Report TR-2000-09, University of Texas, May 2000. A shorter version appeared in *Proceedings of ICNP'00*, Osaka, Japan, November 2000.
- [19] L. Cai, X. Shen, J. Pan, J.W. Mark, Performance analysis of TCP-friendly AIMD algorithms for multimedia applications, *IEEE Transactions on Multimedia* 7 (2) (2005) 339–355.
- [20] L. Wang, L. Cai, X. Liu, X. Shen, AIMD congestion control: stability, TCP-friendliness, delay performance, Tech. Rep., Mar. 2006. <<http://www.ece.uvic.ca/cai/tech-2006.pdf>>.
- [21] L. Wang, L. Cai, X. Liu, X. Shen, Stability and TCP-friendliness of AIMD/RED systems with feedback delays, *Computer Networks* 51 (15) (2007) 4475–4491.
- [22] L. Wang, L. Cai, X. Liu, X. Shen, J. Zhang, Stability analysis of general AIMD/RED systems with multiple bottleneck networks, *Computer Networks* 53 (3) (2009) 338–352.
- [23] S. Liu, T. Basar, R. Srikant, Pitfalls in the fluid modeling of RTT variations in window-based congestion control, in: *Proceedings of the IEEE INFOCOM*, vol. 2, Miami, Florida USA, March 2005, pp. 1002–1012.
- [24] V. Lakshmikantham, S. Leela, A.A. Martynuk, *Practical Stability of Nonlinear System* World Scientific, Nov. 1990, ISBN: 9810203519.
- [25] V. Lakshmikantham, X. Liu, *Stability Analysis in Terms of Two Measures* World Scientific, Feb. 1994, ISBN: 9810213891.
- [26] H.K. Khalil, *Nonlinear Systems*, Prentice-Hall, Upper Saddle River, NJ, 2002.
- [27] S. Floyd and S. McCanne, *Network Simulator*, LBNL public domain software, Available via ftp from <ftp://ftp.ee.lbl.gov>. NS-2 is available in <<http://www.isi.edu/nsnam/ns/>>.



Lijun Wang received the Ph.D. degree in the Department of Applied Mathematics at the University of Waterloo. Her research interests is mainly stability analysis of nonlinear systems and hybrid dynamical systems.



Lin Cai received the M.A.Sc. and Ph.D. degrees (with Outstanding Achievement in Graduate Studies Award) in electrical and computer engineering from the University of Waterloo, Waterloo, Canada, in 2002 and 2005, respectively. Since July 2005, she has been an Assistant Professor in the Department of Electrical and Computer Engineering at the University of Victoria, British Columbia, Canada. Her research interests span several areas in wireless communications and networking, with a focus on network protocol and architecture design supporting emerging multimedia traffic over wireless, mobile, ad hoc, and sensor networks. She serves as the Associate Editor for *IEEE Transactions on Vehicular Technology*, *EURASIP Journal on Wireless Communications and Networking*, and *International Journal of Sensor Networks*.



Xinzhi Liu received the B.Sc. (1982) degree from Shandong Normal University and the M. Sc. (1987) and Ph.D. (1988) degrees from University of Texas, Arlington, Texas (USA). From September 1988 to June 1990, he was with the University of Alberta. Since July 1990, he has been with the Department of Applied Mathematics, University of Waterloo, Canada, where he is a Professor. Dr. Liu's research focuses on stability problems of nonlinear systems, hybrid dynamical systems, monotone iterative methods, and secure communications. Dr. Liu is the author or coauthor of more than 100 research articles and two research monographs and two other books. He is the Chief Editor of *Dynamics of Continuous, Discrete and Impulsive Systems*, Associate Editor for four other journals and an Associate Editor for one series of books and Monographs.



Xuemin (Sherman) Shen received the B.Sc. (1982) degree from Dalian Maritime University (China) and the M.Sc. (1987) and Ph.D. degrees (1990) from Rutgers University, New Jersey (USA), all in electrical engineering. He is a University Research Chair Professor, Department of Electrical and Computer Engineering, University of Waterloo, Canada. His research focuses on mobility and resource management in interconnected wireless/wired networks, UWB wireless communications networks, wireless network security, wireless body area networks and vehicular ad hoc and sensor networks. He is a co-author of three books, and has published more than 400 papers and book chapters in wireless communications and networks, control and filtering. He serves as the Tutorial Chair for IEEE ICC'08, the Technical Program Committee Chair for IEEE Globecom'07, the General Co-Chair for Chinacom'07 and QShine'06, the Founding Chair for IEEE Communications Society Technical Committee on P2P Communications and Networking. He also serves as a Founding Area Editor for IEEE Transactions on Wireless Communications; Editor-in-Chief for Peer-to-Peer Networking and Application; Associate Editor for IEEE Transactions on Vehicular Technology; KICS/IEEE Journal of Communications and Networks, Computer Networks; ACM/Wireless Networks; and Wireless Communications and Mobile Computing (Wiley), etc. He has also served as Guest Editor for IEEE JSAC, IEEE Wireless Communications, IEEE Communications Magazine, and ACM Mobile Networks and Applications, etc. Dr. Shen received the Excellent Graduate Supervision Award in 2006, and the Outstanding Performance Award in 2004 and 2008 from the University of Waterloo, the Premier's Research Excellence Award (PREA) in 2003 from the Province of Ontario, Canada, and the Distinguished Performance Award in 2002 and 2007 from the Faculty of Engineering, University of Waterloo. Dr. Shen is a Fellow of IEEE, and a Distinguished Lecturer of IEEE Communications Society. He is also a registered Professional Engineer of Ontario, Canada.